Journal of Biomedical Optics

SPIEDigitalLibrary.org/jbo

Absorption spectroscopy of single red blood cells in the presence of mechanical deformations induced by optical traps

Michal Wojdyla
Saurabh Raj
Dmitri Petrov

SPIE

Absorption spectroscopy of single red blood cells in the presence of mechanical deformations induced by optical traps

Michal Wojdyla,[a] Saurabh Raj,[a] and Dmitri Petrov[a,b]
[a]Institut de Ciències Fotòniques, Mediterranean Technology Park, Avenida Carl Friedrich Gauss, Num. 3, 08860 Castelldefels, Barcelona, Spain
[b]ICREA—Institucio Catalana de Recerca i Estudis Avancats, Barcelona, Spain

Abstract. The electronic properties of single human red blood cells under mechanical deformations were investigated using a combination of dual beam optical tweezers and UV-vis absorption spectroscopy. The mechanical deformations were induced by two near-infrared optical traps with different trapping powers and trap configurations. The deformations were applied in two ways: locally, due to the mechanical forces around the traps, and by stretching the cell by moving the traps in opposite directions. In the presence of local deformations, the single cell undergoes a transition from an oxygenated state to a partially deoxygenated state. This process was found to be reversible and strongly power-dependent. Stretching the cell caused an opposite effect, indicating that the electronic response of the whole cell is dominated by the local interaction with the trapping beams. Results are discussed considering light-induced local heating, the Stark effect, and biochemical alterations due to mechanical forces, and are compared with reports of previous Raman spectroscopy studies. The information gained by the analysis of a single red blood cell's electronic response facilitates the understanding of fundamental physiological processes and sheds further light on the cell's mechanochemistry. This information may offer new opportunities for the diagnosis and treatment of blood diseases. © *2012 Society of Photo-Optical Instrumentation Engineers (SPIE).* [DOI: 10.1117/1.JBO.17.9.097006]

Keywords: cells; absorption; spectroscopy; lasers in medicine.

Paper 12298 received May 15, 2012; revised manuscript received Aug. 17, 2012; accepted for publication Aug. 20, 2012; published online Sep. 18, 2012.

1 Introduction

The optical trapping of single cells for the analysis of their physical properties can open doors to a range of diagnostic methods with highly specialized targets and provide new insights into several areas of life sciences. Human blood constituents, particularly red blood cells (RBCs), are very important objects of such studies. The RBC, with its simple architecture, can be considered as important for biochemistry as the hydrogen atom is for physics.[1] RBCs are more common than other blood cells and carry information about donor health conditions. As the central component of the circulatory system, RBCs have specific evolved mechanisms for responding to changes in local environment. In the human body, RBCs continuously encounter varied chemical surroundings and also experience large mechanical deformations as they pass through vessels or smaller capillaries with diameters often smaller than the cells themselves. They can survive such repeated passages owing to their high deformability properties. Studies on RBCs under tunable mechanical forces intend to simulate the natural cell environment and can play a crucial role in understanding the cell biological response to mechanical perturbations.[2] It has been shown, for example, that the mechanical properties of RBCs are affected by malaria, spherocytosis, elliptocytosis, or sickle cell anemia.[3]

Sophisticated approaches for RBC analysis combine optical tweezers with spectroscopic techniques like Raman or fluorescence spectroscopy to obtain insight into molecular properties and extract biochemical information at the single-cell level. From a spectroscopic point of view, the most important constituent of RBCs is hemoglobin (Hb), the main role of which, physiologically, is the transport of oxygen from lungs to tissues and participation in the return transport of CO_2 from the tissues to the lungs. This is possible because of the ability of hemoglobin to reversibly bind oxygen with the divalent iron atom of the heme conserving its valence. The chemical state of hemoglobin strongly depends on its local environment and oxygenation state. The Raman technique was used for the study of single RBCs, including investigations on their excitation wavelength[4,5] and environmental effects.[4,6,7] More recently, the direct mechanical perturbation of RBC structure was also investigated via this method.[8–11] One important finding of these studies was the evidence found for mechanically induced cell deoxygenation. Based on this evidence, it can be hypothesized that force induced effects may potentially complement the commonly accepted models describing oxygen binding and release by blood, such as the alkaline Bohr effect, stereochemical mechanism, and heme–heme interactions.[1] Despite the number of such structural (Raman) studies, there is still little known about the electronic properties of hemoglobin at the single-cell level. UV-vis absorption spectroscopy is one of the simplest, label-free techniques yielding direct insight into electronic transitions. Sensitivity of the UV-vis absorption spectroscopy to external perturbations (e.g., temperature, electric field, or pressure) for bulk samples is very well known. It is particularly sensitive to the binding of oxygen by hemoglobin and, therefore, has often been used to monitor oxygenation state transitions in

Address all correspondence to: Dmitri Petrov, ICREA—Institucio Catalana de Recerca i Estudis Avancats, Passeig Lluís Companys, 23 08010 Barcelona, Spain. Tel: 34935534077; Fax: 34935534000; E-mail: Dmitri.Petrov@icfo.es

0091-3286/2012/$25.00 © 2012 SPIE

both bulk hemoglobin solutions[12] and more recently, single RBCs.[13,14] To the best of our knowledge, no study has been conducted on the single RBC's absorption spectroscopy in the presence of external mechanical force.

There are at least two ways to apply deformations with optical traps[8,11] (Fig. 1): by holding the RBC in one or more traps and by stretching the cell using at least two traps. In the first case, the radiation forces attract the cell's constituents with high refractive indices to the trap center, consequently inducing mechanical deformations mainly near the trap (within an area of about 1-μm diameter). In the second case, optical traps additionally stretch the cell by moving in opposite directions. In this case, the deformation also occurs in the part of the cell where no optical beams exist. Studying both local and redistributed cell deformations is important in understanding the interaction of RBCs with tissues. Low-frequency RBC-membrane fluctuations can originate from nonthermal (ATP-driven), internally generated forces.[15] In other words, living cells not only sense external forces but can also actively probe the mechanical properties of their environment by imposing forces. Although the spatial force distributions of these metabolic driven motions largely remain unknown, both localized and distributed mechanosensing is possible.

In this work, we experimentally demonstrated the manner in which specific mechanical deformations induced by optical traps affect the optical absorption of the heme protein within the cell. We propose that the absorption changes are mainly due to mechanical deformations as heating and the Stark effect could not fully explain the observations. We demonstrate a relationship between mechanical stress and electronic response of the cell and propose mechanisms that may be responsible for cell deoxygenation.

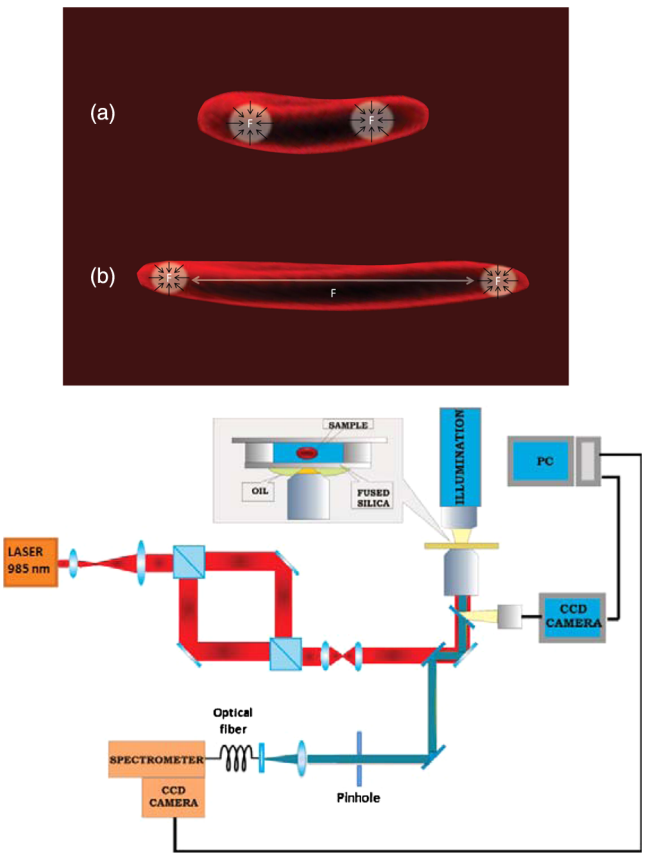

Fig. 1 Top: Two types of deformations which can be applied to the RBC by the optical traps: (a) deformations are applied directly holding RBC in the traps, and (b) the optical traps additionally stretch the cell. Arrows represent hypothetical force (F) distribution. Bottom: Experimental setup.

2 Materials and Methods

The linear optical absorption technique can be combined with optical tweezers using either coherent[16] or incoherent[13] light sources; both these approaches have inherent benefits and drawbacks. Coherent sources, while being quite expensive and spectrally limited, provide very bright and highly focused light to a relatively small volume of a cell. On the other hand, incoherent sources are much cheaper and allow a probe of the overall properties of the whole cell at the expense of lower light intensity and the loss of some quantitative information (e.g., absolute absorbance value).

We used an incoherent broadband source for wide-field illumination of single erythrocytes whose transmittance was monitored in a wide wavelength range using an array detector. The transmitted light intensity was normalized to a signal obtained without the cell present, and the absorption was subsequently calculated. This approach was used to investigate the spectral changes due to the external perturbations induced by the traps themselves and by the cell stretching (see Figs. 1 and 2).

2.1 *Experimental Setup*

The experimental setup comprises a dual-beam optical trapping system combined with an absorption spectrometer (Fig. 1). The optical tweezers setup has been described previously.[8,17] A 985-nm beam was used as a dual trap. The beam was split, expanded, and collimated before it reached the trapping

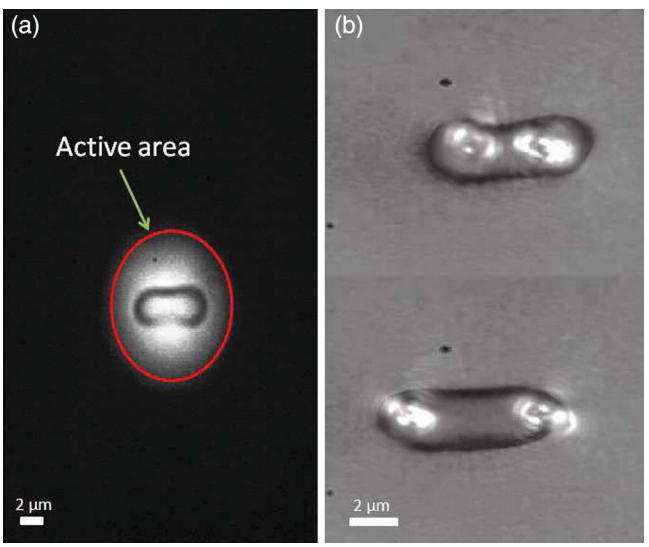

Fig. 2 (a) Image of the single, stretched (20%) RBC recorded in the presence of a 1-mm pinhole in the imaging channel. The brighter part around the cell determines the measured field of view. During the absorption measurements the identical pinhole was used in the spectral channel in order to eliminate the background while the imaging channel was used without the pinhole. (b) Movement of the trapping beams along the cell during typical stretching experiments (here, up to 17%) recorded by removing an IR filter from the imaging channel allowing the detection of IR reflection from the coverslip surface. The stretching leads to an increase in the distance between the trapping beams, and the effective interaction of the cell with the beams is reduced.

objective (100×1.3 numerical aperture oil immersion, Nikon). The back focal plane of the trapping objective was conjugated with movable mirror planes of an interferometer. Movements of the mirrors in either arm of the interferometer result in movements of the traps in the focal plane of the objective without changes in intensity and shape, thus maintaining the trapping potential. The out-of-plane positions of the two trapping beams were controlled by moving one of the lenses in front of the interferometer.

Absorption spectra were recorded using a 150-W halogen lamp (OSL1-EC, Thoralabs) conjugated with a liquid light guide as a probe source. As the light from the lamp is incoherent, it is impossible to focus it to the spot size smaller than the RBC's thickness (about 2 μm). Note that the trapped RBC aligns in the trap and its concavity is normal to the transverse plane. Therefore, we used a wide-field illumination method.[13] The light intensity at the sample was enhanced by passing it through a microscope condenser (20×0.4 NA, Edmund Optics). Cell images after the objective were split by a semitransparent (50/50) mirror. A part of light was then used for imaging the cell while the other part was passed through a 1-mm pinhole to focus it on an optical fiber (600-μm core) coupled with an absorption spectrometer. The main role of the pinhole is to reduce the background light from the area of the cell image [Fig. 2(a)]. The size of the pinhole was optimized to illuminate the entire cell even in its stretched state [see Fig. 2(a)]. The actual position of the (active) field of view (in the spectrometer channel) was determined by absorbing 3-μm beads (Duke Scientific, R0300) and by monitoring changes in the transmittance (in real time, short acquisition time =0.3 s, number of accumulation times =1) of a trapped bead while it approaches the active region. Figure 2(a) shows the field of view obtained by placing the 1-mm pinhole in the imaging channel, thus indicating the actual size of the field of view. During the measurements, the pinhole was removed from the imaging channel and placed in the spectrometer channel, enabling the observation of the whole microscope image during experiments. Consequently, the image shown in Fig. 2(a) was no longer available and the position of the active area had to be determined empirically, for instance, using the beads. Furthermore, the active region did not have a clear boundary, and its size depends not only on the pinhole diameter but also on experimental conditions (intensity of probe light, camera sensitivity). The positions of both traps in the focal plane of the trapping objective were adjusted within the field of view limited by the pinhole. Excellent sensitivity and spectral resolution were obtained using a thermoelectrically controlled Andor charge-coupled device (CCD) camera (DV401A-BV) coupled with a 1200 lines/mm grating spectrometer (Andor, SR163). The camera was cooled down to −60°C and was operated in the full vertical binning (FVB) mode. A second CCD camera (Hamamatsu C3077) provided optical images during stretching experiments. The images were used for calculations of cell deformations. Experiments were performed at room temperature (22°C).

The main difference between our method and the one described in Ref. 13 is that we used a fiber only to guide the transmitted light from the microscope, while in Ref. 13, the fiber also acts as a pinhole (core size 50 μm). We have tested the approach used in Ref. 13 and found it impossible to reduce the active area to a size smaller than the RBC thickness (about 2 μm) even for a very small core size fiber (50 μm) for which the signal-to-noise ratio was already significantly affected. Note that the absorption spectra shown in Ref. 13 are fitted data and not raw data. Hence, we used a much larger pinhole, realizing a better signal-to-noise ratio at the expense of absolute absorbance information.

2.2 *Data Processing*

Relative absorbance was conventionally calculated as $\log(I_0/I)$, where I_0 is the reference signal (recorded in the absence of RBC) and I is the transmitted light intensity, both corrected for the CCD dark signal. As the noncollimated probe beam was used, the absorbance of single cells in a strict sense was not determined but the relative absorbance was calculated. Spectra were recorded separately in two different spectral windows with a total acquisition time of 17 s (for both transmittance and reference signal measurements) and with the baseline corrected. The only exception to this acquisition time was for the measurement in the absence of the traps where such a long detection was not possible. This is because the sample moved out of the field of view, and hence, we could not visualize it for longer than 3 to 5 s (the total acquisition time was 3 to 5 s depending on the sample). Note that a shorter total acquisition time (i.e., lower number of points to average) does not affect the value of the measured relative absorbance (it may only affect the signal-to-noise ratio). In all figures (expect derivative plots), we show the raw data without smoothing or fitting.

We used two traps to hold and stretch the cells during experiments. The deformation of stretched cells was conventionally calculated as $\text{Deformation}(\%) = (\Delta L/L_0) \times 100$, where $\Delta L = L - L_0$ is the difference between the stretched (L) and relaxed (L_0) axial lengths of the cell along the stretching direction.

2.3 *Sample Preparation*

A blood sample of about 50 μl from a healthy human donor was washed three times in Alsever's solution by centrifugation (3 min each at 2000 rpm). The settled precipitate was diluted in 1000 μl of Alsever's solution and stored at 4°C. The stock solution was used within two days to ensure that most of the cells were in viable conditions. The samples for measurements were prepared by dissolving 20 μl of stock solution in 1000 μl of buffer; these samples were injected into a custom-made fluid chamber with precise, stepmotor-driven flow control. The chamber was placed on an inverted microscope with a micrometer-controlled stage.

3 Results

3.1 *Effects of Local Deformation on Absorption Spectra*

Let us first consider the changes in absorption when the cell is held in the optical traps but no stretching is applied [Fig. 1(a)]. Figure 3 shows the representative UV-vis absorption spectra of a single RBC in the absence and presence of optical traps with different total trapping powers (up to 12.9 mW). The spectra of the single RBCs show characteristic electronic bands typical of oxy-hemoglobin. The Soret (or B) band located at 410 nm is followed by the Q band centered at 575 nm and its vibronic repetition at about 540 nm. The hemoglobin spectra are dominated by the heme group and are usually interpreted on the basis of the molecular orbital or the density functional theory (DFT) of metalloporphyrins. According to these calculations, the Q

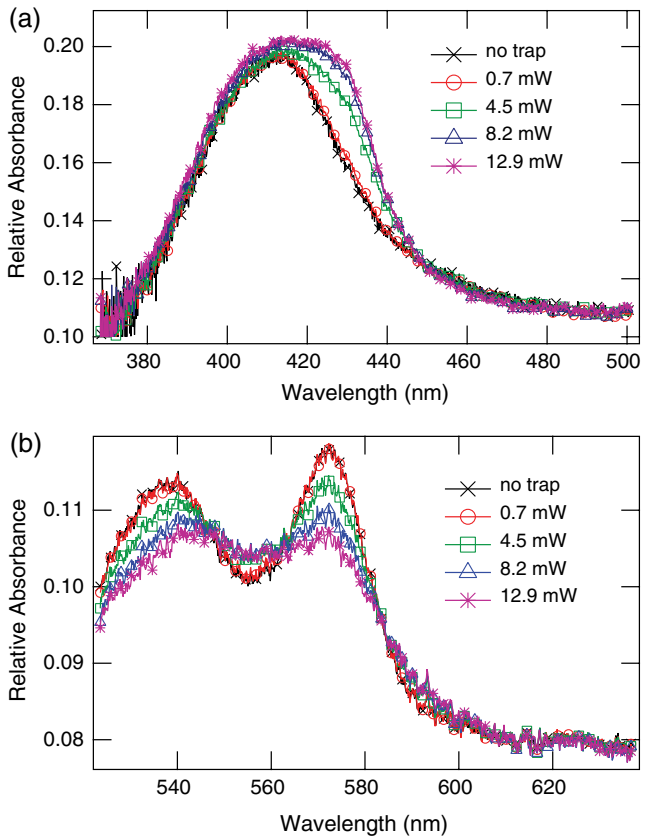

Fig. 3 Optical trap effect on the absorption spectra of the single RBC in the region of the (a) Soret and (b) Q bands measured at different trapping powers. The observed spectral changes are reversible.

and Soret bands are mainly attributed to the π-to-π^* transitions between $e_g \leftarrow a_{1u}$ and $e_g \leftarrow a_{2u}$, respectively.[18]

To record the spectra in the absence of the traps, the cell was initially trapped using low power (0.7 mW), and the trapping beams were switched off for a short time (about 3 to 5 s) to allow the spectra recording without noticeable (controlled by imaging) cell displacements or rotations. The cell was then retrapped and the spectra were recorded with the same cell at increasing power. To avoid the photodegradation, the trapping beams were always switched off during power adjustment. For the same reason, the power-dependent measurements were recorded only at a given distance between the trapping beams (about 3 μm). At this distance, the RBC membranes were not stretched, as observed via imaging. However, it is probable that relative locations of the beams affect the cell state at least via redistribution of stresses within the cell. Different cells were used for measurements in the Soret and Q spectral windows but following the same procedure.

The spectra (Fig. 3) are found to be strongly dependent on the power of the traps. At low power (0.7 mW), the trap effect on the spectra is almost negligible. At higher powers of the trapping beams, a significant drop in the Q band intensity close to the absorbance maxima occurs with a simultaneous increase in absorbance at about 560 nm. This effect is accompanied by the red shift (about 5 nm at maximal power) of the vibronic band and a slight Q band broadening. A different behavior is observed in the Soret band, which becomes strongly inhomogeneous, suggesting the appearance of a new band (at about 430 nm); the appearance of this band is confirmed via fitting analysis (data not shown). The inhomogeneity of this band in the presence of traps is clearly visible but a possible contribution of the increase in power to the broadening of the native band with power cannot be disregarded. The observed spectral changes should be measurable using the single trap. The main advantage of the two traps is that all degrees of freedom of the RBC motion are well constrained, preventing eventual cell reorientation, especially when turning the trapping beams on and off. Moreover, two-point trapping is favorable over a single trap because the energy of the beams is partially distributed over the cell. Hence, we approximately double the volume of interaction with the beams by simultaneously reducing the other effects such as local heating.

Control experiments were performed by repeatedly cycling between low (0.7 mW) and high trapping powers to check the reversibility of the absorbance changes and determine the degree of photodamage. We found that the spectra regain the previous shape when the trap power is reduced [Fig. 4(a)]. This also indicates that the cells are not photodamaged at the optical powers and exposure times used, as confirmed by an additional test experiment when the absorption spectra were measured over 99 s of continuous illumination [Fig. 4(b)]. At longer illumination times, the cell slowly starts to degrade, as is reflected in the decrease (with time) in the integral intensities

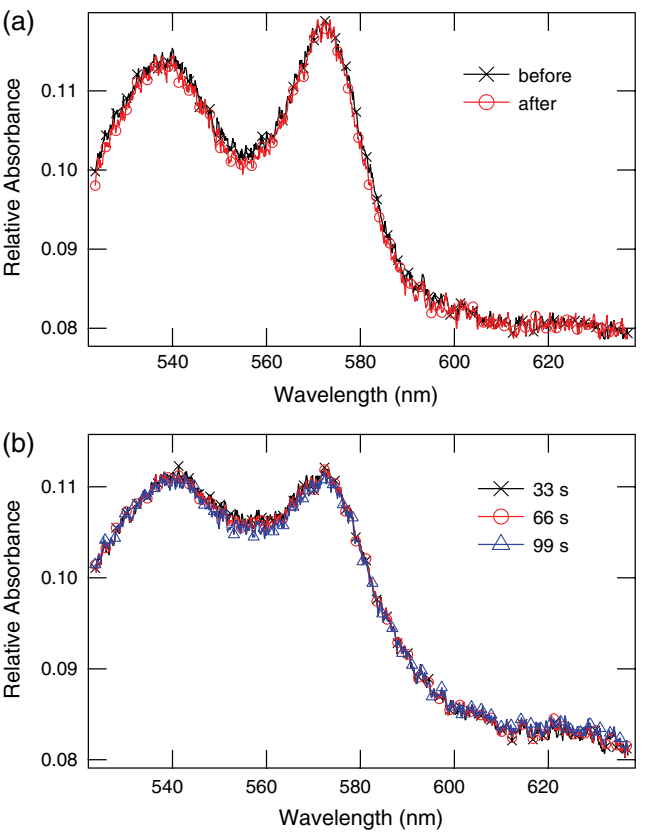

Fig. 4 (a) The photostability of the RBCs monitored via the Q absorption band recorded (at 0.7 mW) before (black line and crosses) and after (red line and circles) three consecutive 17 s scans with variable trapping powers. (b) Absorption spectra of the cell recorded continuously over initial 33 s (black line and crosses), after 66 s (red line and circles), and 99 s (blue line and triangles) at 8.2 mW. The acquisition time for each spectrum is 33 s, and spectra are taken without time delay. There are no significant changes in spectra indicating that the sample is photostable at these trapping powers and exposure times.

of both the Q and Soret bands (data not shown). The presence of traps leads to the evident increase of the Soret band intensity at 430 nm with power; hence, photodecomposition can be excluded in this case. The presented changes in the absorption spectra are therefore due to the effect of the trapping beams on the cell. Similar trap-induced effects were observed for 20 cells.

3.2 *Effects of Distributed Deformation*

Now we consider the overall effect when both the local deformation and the stretching are applied to the cell [Fig. 1(b)]. The corresponding absorption spectra for single cells at relaxed and stretched states are presented in Fig. 5. This figure shows that the stretching of the cell causes opposite effects on the absorption spectra that are induced with the increase of the trap power: the Q band intensity increases close to its maxima with a simultaneous decrease of absorbance at about 560 nm. Both the Q and Soret bands become narrower, and with stretching, two distinct bands are clearly resolved in the Q band. This effect is reversible (see Fig. 5). Such spectral behavior, which is opposite of the previous case, suggests that the stretching reduces the interaction of the cell with trapping beams. In order to confirm this hypothesis, a stretching experiment was conducted for the cell trapped near the coverslip surface, enabling the monitoring of the relative positions of two trapping beams [see Fig. 2(b)]. This was possible by removing the IR blocking filter from the imaging channel and recording the image of the IR light reflected from the coverslip surface. The image indicates that the overall overlap of the trapping beams with the cell is strongly reduced with a possible slipping of the traps along the cell with stretching. Consequently, the absorption spectra of the cell tend to restore the previous unperturbed shape. This behavior is reproducible from cell to cell for 40 studied cells stretched even as high as 33%.

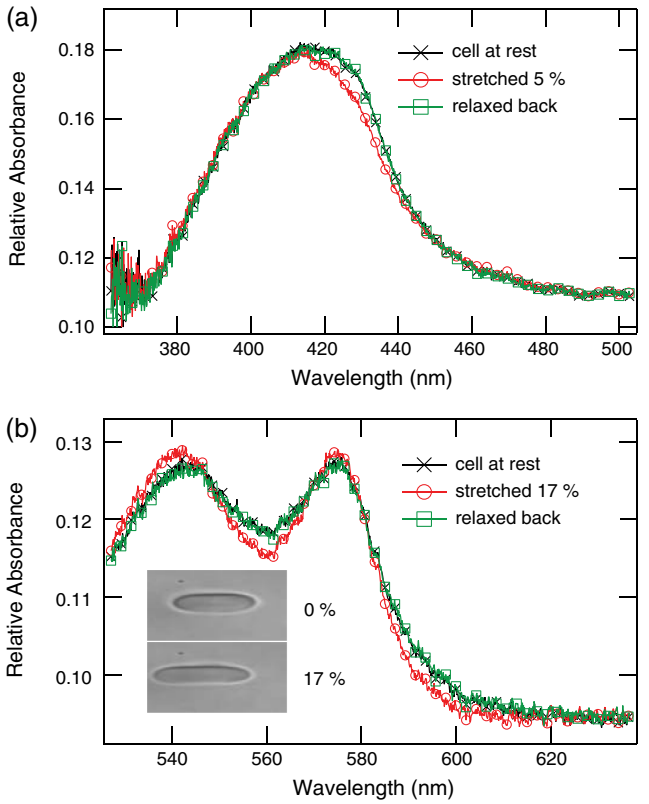

Fig. 5 Absorption spectra of a single RBC in the (a) Soret and (b) Q bands for the relaxed (black lines and crosses) and stretched (red lines and circles) cells (power 4.5 mW). This effect is reversible: the absorption spectra of cells relaxed back after stretching (green lines and squares) are almost identical to the initial spectra. The inset in Fig. 5(b) shows images of the relaxed and stretched (17%) cell.

The reasons for the difference in the relative absorption among cells can be partly explained by the variation in the size of the cells and/or Hb concentration. For example, the higher value of relative absorbance in Fig. 5(b) as compared to that in Fig. 3(b) (at 4.5 mW) is attributed to the difference in size [larger cell shown in Fig. 5(b)]. Similarly, we can explain the differences between the plots in Figs. 3(b) and 4(b) (at 8.2 mW) by size.

4 Discussion

The above absorption spectroscopy studies show that RBCs possess a complex absorption behavior with the possible formation of new (deoxy) species. This behavior can be driven by various processes as the electronic structure of heme and other metalloporphyrins is sensitive to external perturbations. The observed trap-induced absorption changes can potentially result from: 1. trapping light-induced heating, 2. the Stark effect (both due to the high intensity of trapping light), and 3. chemical alterations induced by optical forces. Below we consider each of these effects in details.

4.1 *Optical-Beam-Induced Heating*

In the optical tweezers experiments, the optical beams are tightly focused, resulting in large intensities at their focused area and the consequent possible heating due to light absorption in the neighborhood of the focused area. In the simplest case of a trapped single micron-sized polystyrene or silica particle, the most important contribution to heating is from light absorption in the solvent around the particle and not in the particle itself.[19] Water is heated more than the polystyrene particle due to its higher extinction coefficient (14 m^{-1} for water versus 6 m^{-1} for polystyrene beads at 1064 nm). The estimated temperature increase due to water heating was about 8°C/W.[19] This increase leads to about a 0.1°C jump in our experiment at 12.9 mW. For comparison, this value of temperature increase is measured to be ~15°C/W and 12°C/W for micron-sized spherical liposome vesicles having bilayer membranes and for Chinese hamster ovary (CHO) cells, respectively (as measured using Stokes-shifted fluorescence).[20] Here, the liposome absorption is assumed to also be governed by absorption in water. The situation is more complicated for RBCs. The molar extinction coefficient of HbO_2 at 985 nm is about 1112 $M^{-1}cm^{-1}$,[21] and the mean corpuscular Hb concentration in cells is about 5 $mmol/L$.[22] Multiplying these values yields the RBC extinction coefficient of about 556 m^{-1}, which is significantly higher than that for water. Exact calculations of the temperature increase in RBC are quite complicated and beyond the scope of this work. Nevertheless, we roughly estimated a possible temperature increase, assuming a direct proportionality of the extinction coefficient and heating factor. Multiplying the RBC-to-water extinction coefficient ratio (at 985 nm) and the highest reported heating factor for water (15°C/W), we estimated that the maximal increase of temperature in our experiments should not exceed 0.5°C, 3°C, 5°C, and 8°C for 0.7, 4.5, 8.2, and 12.9 mW, respectively. Note that these obtained values are upper limits and correspond to the case where the total

absorbed (via RBC) light converts to heat (no dissipation). A better estimation would require the solution of the heat transport differential equation for a strongly heterogenous system (like RBC) or direct temperature measurements, ideally with a sensor placed inside the cell.

To the best of our knowledge, the temperature dependence of absorption spectra for a single cell has not yet been studied. For solutions, such data are available at relatively high concentrations.[23] A prominent effect of the temperature increase from 20°C to 40°C was a small decrease in the absorptivity of oxy-, carboxy-, and deoxyhemoglobin in the Q band region but only near the absorbance maxima. The effect was more pronounced for HbO_2 than for Hb. Despite the fact that the temperature jump was 20°C, the drop in the absorbance maxima was much smaller than that observed in our measurements. More importantly, in contrast to our experiments, the spectra shape was almost the same, and no noticeable changes in absorptivity was observed with the temperature increase at 560 nm. We observed a strong and instantaneous reversible effect at low power (4.5 mW); hence, it is unlikely that this is caused solely by a thermal effect when temperature rise of <3°C is expected. Another argument against the temperature jump explanation is the evidently growing (with the power of the traps) integral intensity of the Soret band. An exactly opposite behavior is expected with the temperature increase, mainly due to phonon coupling (see e.g., Refs. 24 and 25). In addition, a simple thermal broadening of the Soret band cannot justify the observed changes since a new band (at higher powers) becomes strongly inhomogeneous.

All the above arguments indicate that the local heating, even though it cannot be completely excluded, has a rather secondary effect on our measurements. In other words, the heating caused by the traps may facilitate the decrease of absorption near the Q bands maxima (or broadening) to some extent but it cannot be considered the sole explanation of the observed behavior.

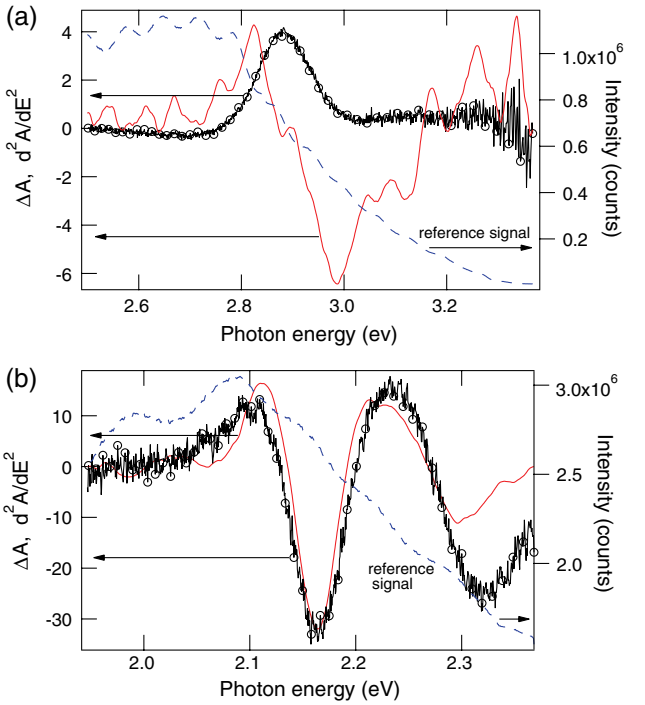

Fig. 6 Comparison of the second derivative of the absorption spectra in the absence of the traps (red lines) with difference spectrum (black lines and circles) in the region of the (a) Soret and (b) Q bands. Raw data were smoothed using a smoothing spline technique before the derivative calculation. The difference spectra were obtained by the subtraction of the spectra in the presence (8.2 mW) and absence of the traps, and multiplied by 150 and 4000 in the the Soret and Q range, respectively, for comparison with the second derivative. Characteristic oscillations in the derivative plots, which are particularly strong in the the Soret region, are due to interference effects enhanced by numerical differentiating (see also plots of the reference signal:blue dashed lines).

4.2 *Stark Effect*

Another potential mechanism is associated with the Stark effect near the focus of the traps. The tightly focused beam gives rise to intensities on the order of MW/cm^2 even for beams of several milliwatts. Based on the assumption of a diffraction limited spot size, the electric field strength at the focus point is on the order of $10^6\ V/m$. The effect of such large electric fields should be considered, particularly in absorption measurements. The electric field may perturb the charge distribution directly (Stark effect) or deform cells via the field-induced polarization and consequently change the protein conformation. In general, the Stark effect might result in shifts of all optical transition frequencies and redistribution of oscillator strengths. It may also result in the access to transitions that are normally forbidden (by selection rules) or the splitting of degenerate energy levels. According to the perturbation theory, the Stark spectrum (ΔA) line shape is proportional to the second derivative of the absorption spectrum.[26] We calculated this function in the absence of the traps, and the derivative spectra were compared with difference spectra shown in Fig. 6. While the similar shapes of derivative and difference spectra were obtained in the Q band, there is a considerable disagreement in the Soret band. We found that the difference spectrum, particularly in the Soret spectral range, differs significantly from the previously reported Stark spectra of deoxymyoglobin.[27] The Soret band is due to the presence of Hb in its native form and it is very sensitive to alterations in the surrounding environment.[28] A strong disagreement of the difference spectra with both the derivative and Stark spectra[27] indicates that the Stark effect hypothesis appears to break down and it cannot alone explain the changes observed in the experimental spectra.

4.3 *Mechanical Deformation*

Now we consider how the mechanical deformations of the cell induced by the trapping beams may change the RBC absorption spectra. The measured absorption bands originate from the heme groups embedded in a hydrophobic protein backbone with characteristic conformation. The changes in the shape and position of absorption bands could therefore indicate possible conformational changes of the surrounding proteins. The permanent damage of proteins (e.g., unfolding or denaturation[28]) can be excluded as the process is completely reversible. There are well-known reversible conformational changes that accompany Hb oxy-deoxy transitions.[29] The oxy and deoxy forms of hemoglobin possess different absorption spectra (particularly in the Q band region) since the binding of oxygen rearranges the electronic distribution and alters the orbital energy. The spectra of oxy-hemoglobin are dominated by two distinct peaks in the visible (Q) range, as is shown in Fig. 3 for a single cell in the absence of the traps. In contrast, the deoxy-hemoglobin or deoxygenated erythrocytes (e.g., sodium dithionite treated) exhibit a single broad band centered at about 560 nm.[13,21] In normal

conditions, the cells have a mixture of oxygenated, deoxygenated, and partially deoxygenated forms of Hb, which coexist within a delicate balance, depending on the chemical surrounding (e.g., pH, O_2 partial pressure, membrane tension). Our power dependence studies show that the intensity ratio of deoxy peaks to that of oxy peaks (A_{560nm}/A_{575nm}) increases with the trapping power. This behavior is expected when a partial conversion of the cell from the oxygenated state to deoxygenated state occurs. An evidence of the partial cell deoxygenation is also clearly visible in the Soret region where the red-shifted absorption appears with the power increase, leading to the strong band inhomogeneity. These results are consistent with the well-known change in the quaternary structure that accompanies the hemoglobin deoxygenation.[1] The optical traps induce mechanically conformational changes of the proteins leading to the oxygen release. The varying degree of cell deoxygenation can be obtained by adjusting the power of the traps. These results and interpretation agree well with similar Raman studies where power-dependent, reversible, optical-trap-induced partial cell deoxygenation was observed.[11] The data clearly indicate that the effect also completely dominates the cell's electronic response. The physical picture describing the observed local effect seems to be complex, and direct theoretical predictions are not available yet. We hypothesize that optical forces deform the proteins mechanically by attracting different cell constituents (including membrane, cytoskeleton, and cytosol) leading to the increase in neighbor–neighbor (Hb–Hb), Hb–membrane, or Hb–cytoskeleton interaction and forcing hemoglobin conformational changes.[8,11] The observed local effect can be also directly related to the folding of RBCs in the presence of an optical trap (power dependent process).[30] Even if forces are applied locally [Fig. 1(a)], they are accompanied by the redistributed deformation of the whole membrane, since the trapping leads to significant changes of the RBC shape (from the normal biconcave disk shape into a rod-like shape). Such folding can result in the mechanical squeezing of the cytosol and cytoskeleton inside the cell. Note that, in principle, any change in the RBC shape may potentially affect Hb mechanically since the Hb binds with the inner wall of the RBC membrane (with possible intercalation)[31,32] as well as to the entire cytoplasmic domain of band 3 (see Ref. 33) and spectrin (see Refs. 34 and 35). An explanation beyond these qualitative arguments will have to await further experiments. In particular, the role of the cell folding remains to be elucidated. The study of the time evolution of absorption bands in the presence of external perturbation can further clarify this issue (the folding and unfolding of RBCs are relatively slow processes[30]). Time-resolved absorption measurements of a single RBC are planned for further research.

To further explore the potential role of the membrane shape on the chemical state of hemoglobin, we performed stretching experiments where the membrane was intentionally deformed with two traps moving apart. The obtained results indicate that the membrane stretching apparently does not lead to cell deoxygenation. On the contrary, a higher degree of the overall cell oxygenation is evident. This behavior can be explained by reduced interaction of the cell with the trapping beams. Stretching can also result in cell unfolding, which in turn may facilitate cell oxygenation. These observations at first glance are in contrast to previous Raman experiments[8,36] where it was found that the deoxygenation of RBC occurs with membrane stretching. There are a few reasons to explain this apparent discrepancy. The Raman and absorption spectroscopic results differ due to different experimental realizations and sensitivities. We suppose that the stretching-induced deoxygenation is a much weaker effect occurring locally in the cell, and hence, the absorption measurements are completely masked by the above described local interaction with trapping beams. The confocal Raman spectroscopy probes a limited volume inside the cell while the wide-field illumination during the absorption measurement yields the response of the whole cell. As we have reported, the presence of the optical traps leads to partial cell deoxygenation, monitored via the absorption changes. However, this deoxygenation is presumably not evenly distributed over the whole cell but dominates in the regions close to the traps, leaving other parts of the RBC in their initial oxygenated state [see Fig. 2(b)]. In the case of total cell deoxygenation, we see in the absorption spectra, the full oxy → deoxy cell conversion with a distinct peak at 560 nm, but this is not the case here. Since the Raman spectroscopy experiment probed the cell's region between the traps, the hemoglobin in the focal volume was initially in the oxy state (not or slightly affected by the above described local traps effect). Therefore, stretching-induced deoxygenation was observed. In addition, Raman signals usually suffer from an excessive bias toward the surface layers of probed samples. This might prevent the observation of the signals from deeper layers of the probed RBCs, confining their responses to only shallow layers close to the membrane. The regions close to the membrane presumably undergo maximal deformations with stretching and can strongly contribute to the Raman signal. In contrast, the absorption spectroscopy method used here probed the whole cell, and no evidence was found for overall cell deoxygenation with membrane stretching. The changes in the absorption spectra are dominated by the direct interaction of the cells with the traps, which masks a weaker stretching effect (note that, in practice, the sensitivity of Raman spectroscopy can be better than the sensitivity of absorption since the background signal is much lower). However, based on the results presented here, it is evident that the overall (total) cell deoxygenation does not occur with the membrane stretching. The oxy → deoxy transitions analyzed in Ref. 8 can therefore only be a partial effect occurring locally in the cell, most likely close to the membrane.

Future experiments should be aimed at combining the absorption and Raman spectroscopy with optical tweezers in one experimental setup and simultaneously monitoring the spectra of the same cells in identical experimental conditions (solvent, stretching state, etc.) using polystyrene beads biochemically attached to the cell membrane.

5 Conclusion

In summary, the absorption spectra showed that single RBCs undergo a partial deoxygenation in the presence of local deformations induced by trapping beams; this result is consistent with the reports of previous Raman spectroscopy studies. The effect was found to be strongly dependent on the trap power and fully reversible. We showed that the local heating and Stark effect cannot justify the observed changes in the optical absorption. Therefore, mechanically induced chemical alterations (including Hb conformational changes) are the most important contributions. The absorption response of the trapped cell is dominated by the local interaction with the optical traps, as confirmed by the stretching experiments. The changes in absorption of the stretched RBC were explained by the decrease in the effective overlap and resulting interaction of the cell with the

trapping beams. There is no evidence in the absorption measurements for the overall deoxygenation of the whole cell with membrane stretching, although localized deoxygenation near the membrane cannot be disregarded. Such localized deoxygenation may facilitate the oxygen exchange with tissue.

Radiation forces that attract cell constituents to the trap center or directly stretch its membrane may simulate the real distribution of the deformations that cells experience as they squeeze through smaller microcapillaries or actively interact with the tissue.

Acknowledgments

We acknowledge the financial support from Fundació Privada Cellex Barcelona and the Spanish Ministry of Science and Innovation (MICINN FIS2008-00114, FIS2011-24409).

References

1. M. F. Perutz, *Mechanisms of Cooperativity and Allosteric Regulation in Proteins*, Cambridge University Press, Cambridge, United Kingdom (1990).
2. G. Bao and S. Suresh, "Cell and molecular mechanics of biological materials," *Nature Mater.* **2**(11), 715–725 (2003).
3. S. Suresh, "Mechanical response of human red blood cells in health and disease: some structure-property-function relationships," *J. Mater. Res.* **21**(8), 1871–1877 (2006).
4. B. R. Wood, B. Tait, and D. McNaughton, "Micro-Raman characterisation of the *R* to *T* state transition of haemoglobin within a single living erythrocyte," *Biochim. Biophys. Acta.* **1539**(1–2), 58–70 (2001).
5. A. Bankapur et al., "Raman tweezers spectroscopy of live, single red and white blood cells," *PLoS ONE* **5**(4), e10427 (2010).
6. K. Ramser et al., "A microfluidic system enabling Raman measurements of the oxygenation cycle in single optically trapped red blood cells," *Lab Chip* **5**(4), 431–436 (2005).
7. B. R. Wood et al., "Resonance Raman spectroscopy of red blood cells using near-infrared laser excitation," *Anal. Bioanal. Chem.* **387**, 1691–1703 (2007).
8. S. Rao et al., "Raman study of mechanically induced oxygenation state transition of red blood cells using optical tweezers," *Biophys. J.* **96**(1), 209–216 (2009).
9. S. Rao et al., "Polarization Raman study of protein ordering by controllable RBC deformation," *J. Raman Spectrosc.* **40**(1), 1257–1261 (2009).
10. S. Raj et al., "Mechanochemistry of single red blood cells monitored using Raman tweezers," *Biomed. Opt. Express* **3**(4), 753–763 (2012).
11. R. Liu et al., "Power dependent oxygenation state transition of red blood cells in a single beam optical trap," *Appl. Phys. Lett.* **99**(4), 043702 (2011).
12. W. G. Zijlstra, A. Buursma, and W. P. Meeuwsen-van Der Roest, "Absorption spectra of human fetal and adult oxyhemoglobin, de-oxyhemoglobin, carboxyhemoglobin, and methemoglobin," *Clin. Chem.* **31**(9), 1633–1638 (1991).
13. A. Alrifaiy and K. Ramser, "How to integrate a micropipette into a closed microfluidic system: absorption spectra of an optically trapped erythrocyte," *Biomed. Opt. Express* **2**(8), 2299–2306 (2011).
14. J. Y. Lee et al., "Absorption-based hyperspectral imaging and analysis of single erythrocytes," *IEEE J. Sel. Top. Quant. Electron.* **18**(3), 1130–1139 (2011).
15. T. Betz et al., "ATP-dependent mechanics of red blood cells," *Proc. Natl. Acad. Sci. U. S. A.* **106**(36), 15312–15317 (2009).
16. I. Itzkan et al., "Confocal light absorption and scattering spectroscopic microscopy monitors organelles in live cells with no exogenous labels," *Proc. Natl. Acad. Sci. U. S. A.* **104**(44), 17255–17260 (2007).
17. S. Rao et al., "Single DNA molecule detection in an optical trap using surface-enhanced Raman scattering," *Appl. Phys. Lett.* **96**(21), 213701 (2010).
18. M. Gouterman, G. H. Wagniere, and L. C. Snyder, "Spectra of porphyrins: part II. four orbital model," *J. Mol. Spectrosc.* **11**(1–6), 108–127 (1963).
19. E. J. G. Peterman, F. Gittes, and C. F. Schmidt, "Laser-induced heating in optical traps," *Biophys. J.* **84**(2), 1308–1316 (2003).
20. Y. Liu et al., "Evidence for localized cell heating induced by infrared optical tweezers," *Biophys. J.* **68**(5), 2137–2144 (1995).
21. S. Prahl, "Optical absorption of hemoglobin," Oregon Medical Laser Center, http://omlc.ogi.edu/spectra/hemoglobin (1998).
22. M. C. Van Beekvelt et al., "Performance of near-infrared spectroscopy in measuring local O_2 consumption and blood flow in skeletal muscle," *J. Appl. Physiol.* **90**(2), 511–519 (2001).
23. J. M. Steinke and A. P. Shepherd, "Eftects of temperature on optical absorbance spectra of oxy-, carboxy-, and deoxyhemoglobin," *Clin. Chem.* **38**(7), 1360–1364 (1992).
24. L. Cordone et al., "Optical absorption spectra of deoxy- and oxyhemoglobin in the temperature range 300–20 K: relation with protein dynamics," *Biophys. Chem.* **24**(3), 259–275 (1986).
25. A. Di Pace et al., "Protein dynamics: vibrational coupling, spectral broadening mechanisms, and anharmonicity effects in carbonmonoxy heme proteins studied by the temperature dependence of the Soret band lineshape," *Biophys. J.* **63**(4), 475–484 (1992).
26. R. N. Frese et al., "Electric field effects on the chlorophylls, pheophytins, and -carotenes in the reaction center of photosystem II," *Biochemistry* **42**(30), 9205–9213 (2003).
27. S. Franzen et al., "Stark-effect spectroscopy of the heme charge-transfer bands of deoxymyoglobin," *J. Phys. Chem. B* **103**(16), 3070–3072 (1999).
28. M. Mahato et al., "Hemoglobin-silver interaction and bioconjugate formation: a spectroscopic study," *J. Phys. Chem. B* **114**(20), 7062–7070 (2010).
29. M. F. Perutz, *Methods of Multivariate Analysis*, John Wiley and Sons, New York (2002).
30. A. Ghosh et al., "Euler buckling-induced folding and rotation of red blood cells in an optical trap," *Phys. Biol* **3**(1), 67–73 (2006).
31. N. Shaklai, J. Yguerabide, and H. M. Ranney, "Interaction of hemoglobin with red blood cell membranes as shown by a fluorescent chromophore," *Biochemistry* **16**(25), 5585–5592 (1977).
32. S. Fischer et al., "The binding of hemoglobin to membranes of normal and sickle erythrocytes," *BBA Biomembranes* **375**(3), 422–433 (1975).
33. J. A. Walder et al., "The interaction of hemoglobin with the cytoplasmic domain of band 3 of the human erythrocyte membrane," *J. Biol. Chem.* **259**(16), 10238–10246 (1984).
34. S. C. Liu and J. Palek, "Hemoglobin enhances the self-association of spectrin heterodimers in human erythrocytes," *J. Biol. Chem.* **259**(18), 11556–11562 (1984).
35. A. Chakrabarti et al.," Oxidative crosslinking, spectrin and membrane interactions of hemoglobin mixtures in HbEbeta-thalassemia," *Hematology* **13**(6), 361–368 (2008).
36. G. Rusciano, "Experimental analysis of Hb oxy-deoxy transition in single optically stretched red blood cells," *Phys. Medica* **26**(4), 233–239 (2010).